DOI: 10.1002/ejic.200900813

Complexes with Sterically Bulky Allyl Ligands: Insights into Structure and Bonding

Stephen C. Chmely[a] and Timothy P. Hanusa*[a]

Keywords: Solid-state structures / Main group elements / Transition metals / Allyl complexes / Steric bulk

The allyl anion $[C_3H_5]^-$ is often found in combination with other ligands in organometallic complexes. Compounds in which allyl groups are the only or principal type of ligand, however, are often coordinatively unsaturated and prone to decomposition. It is possible to increase the thermal and sometimes oxidative stability of such complexes by adding sterically bulky substituents (e.g., $–SiMe_3$) to the allyl group. Main group, transition metal, and f-element compounds constructed with bulky allyl ligands display a wide range of monomeric, oligomeric, and polymeric structures. Some of these complexes have no counterparts with unsubstituted allyl groups, and others are active polymerization catalysts. Research in this area has served to expand the range of structural types and bonding that can be incorporated into metal allyl chemistry.

Introduction

The allyl anion, $[C_3H_5]^-$, is among the smallest π-delocalized ligands found in organometallic chemistry. Its compact size contributes to its conformational flexibility; it binds to metals in both bridged (η^3) and "classic" σ- (η^1) modes, and interconversion between them can be rapid. In combination with a wide variety of other ligand types (e.g., halides, phosphanes, carbonyls, and cyclopentadienes), allyl anions have been incorporated into complexes from across the periodic Table (the s-, p-, d-, and f-block are all represented).[1]

[a] Department of Chemistry, Vanderbilt University, Nashville, Tennessee, 37245, USA
Fax: +1-615-/343-1234
E-mail: t.hanusa@vanderbilt.edu

Despite its versatility, the small size of the allyl ligand can be a liability in many contexts, especially in homoleptic complexes, $M(C_3H_5)_n$. With a few important exceptions [e.g., the bis(allyl) complexes of Ni, Pd, and Pt, which are valuable in organic synthesis],[2] most $M(C_3H_5)_n$ compounds are poorly studied and infrequently used. A major reason for this is that metal centers in homoleptic allyl complexes are often coordinately unsaturated, and low-energy pathways for decomposition are available. As a result, many of them are thermally unstable and difficult to handle. Wilke cites examples of these in his early review of homoleptic allyl complexes:[3] especially notable are $Fe(C_3H_5)_3$ and $Co(C_3H_5)_3$, which decompose above –40 °C, $V(C_3H_5)_3$, which explodes above –30 °C, and $Zr(C_3H_5)_4$, $Nb(C_3H_5)_4$, and $Ta(C_3H_5)_4$, all of which decompose at 0 °C. Even $Ni(C_3H_5)_2$ decomposes within a day at room temperature under a nitrogen atmosphere.

Stephen C. Chmely was born in Memphis, Tennessee, and received his bachelor's degree in chemistry from Western Kentucky University in 2006. He is currently a graduate student at Vanderbilt University in Nashville, Tennessee, working in the group of T. P. Hanusa on the chemistry of sterically augmented allyl complexes and phosphonium substituted ligands.

Timothy P. Hanusa was born in Council Bluffs, Iowa, and received his bachelor's degree in chemistry from Cornell College in 1978. He received his Ph.D. degree in Inorganic Chemistry from Indiana University, Bloomington, under the direction of Lee J. Todd. After a postdoctoral appointment with William J. Evans at Irvine, California, he joined the chemistry faculty at Vanderbilt University in Nashville, Tennessee, in 1985, where he is now Professor of Chemistry. His research has focused on organometallic complexes of the main group elements and on magnetically variable compounds of the transition metals.

By occupying larger areas of the metal coordination sphere and physically blocking decomposition routes, sterically bulky ligands have often been used to improve the kinetic stability of organometallic complexes. Cyclopentadienyl chemistry has long benefited from the use of such substituted rings as C_5Me_5 and $C_5H_3(SiMe_3)_2$, which can be used to synthesize compounds of greater diversity and stability than is possible with Cp alone.[4–6] A similar approach is effective with the allyl ligand. The allyl anion can be substituted with a variety of alkyl, aryl, silyl, and siloxide groups, all of which can have substantial effects on the properties of their associated compounds. For example, methylated allyl ligands are known to provide modest improvements in the thermal stability of complexes,[7] and the bulky nickel allyl complex Ni(1,1′,3,3′-$Ph_4C_3H)_2$ is stable at room temperature.[8] The first widespread studies of the changes in properties that could be conferred on allyl complexes with the use of sterically bulky ligands involved trimethylsilylated ligands. Fraenkel reported the synthesis of lithiated derivatives of $[(SiMe_3)_nC_3H_{5-n}]^-$ anions in the early 1990s,[9–11] and allyl ligands with one to three trimethylsilyl substituents are known.[12] These and related variants such as dimethyl(*tert*-butyl)silylallyl[13] have remained the most extensively used ligand types in bulky allyl complex chemistry. The trimethylsilyl groups provide good solubility in hydrocarbon solvents, and substantially increase the size and steric demands of the ligands; e.g., at 216 Å^3, the *syn*,*syn*-$[1,3\text{-}(SiMe_3)_2C_3H_3]^-$ anion has 4 times the volume of the parent $[C_3H_5]^-$ ion (54 Å^3) (Figure 1).[14]

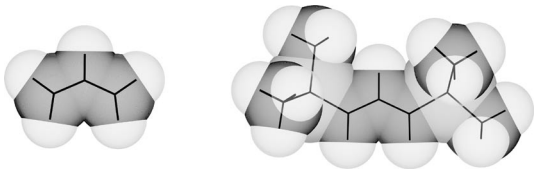

Figure 1. Space-filling models of $[C_3H_5]^-$ (left) and $[1,3\text{-}(SiMe_3)_2C_3H_3]^-$.

How much of an effect such increased bulk has on the properties of the association complexes varies not only with the degree of substitution, but also with the identity of the substituent. The energetic barrier for displacing silyl-based substituents from the plane of a delocalized anion is lower than for hydrocarbyl groups,[15] and such bending effectively reduces the steric impact of the group. Consequently, a single substituent may have minimal effect on the structure of the complex (e.g., as discussed below, $[Cr(C_3H_5)_2]_2$ and $\{Cr[1\text{-}(SiMe_3)C_3H_4]_2\}_2$ are related dimers).[16] Conversely, three trimethylsilyl groups on the ligand may not affect structures much more than the presence of two (e.g., $Cr[1,3\text{-}(SiMe_3)_2C_3H_3]_2$ and $Cr[1,1',3\text{-}(SiMe_3)_3C_3H_2]_2$ are comparable monomeric species).[16]

In some cases, substituted allyl ligands provide versions of known compounds that are more robust than the unsubstituted species. For example, unlike the pyrophoric $Ni(C_3H_5)_2$, the trimethylsilylated derivative $Ni[1,3\text{-}(SiMe_3)_2C_3H_3]_2$ only slowly decomposes in air (from hours to days).[17] In addition, the homoleptic thorium complexes $Th[(SiMe_3)_nC_3H_{5-n}]_4$ (n = 1, 2) are stable to 90 °C,[18] in contrast to $Th(C_3H_5)_4$, which decomposes at 0 °C. In other cases, the presence of substituent groups aids in crystallization, so that solid-state structures may be obtained; calculations suggest that the X-ray crystal structure of the lithium dimer $\{Li[1,1',3\text{-}(SiMe_3)_3C_3H_2]\}_2$ is related to that of the unsubstituted complex, which is known to be a dimer from cryoscopy, but which has not been structurally authenticated.[19]

Of even greater interest is the use of substituted allyl ligands to support entirely new classes of metal complexes. Discussed below are the thermally stable, electron-deficient transition metal bis(allyl) compounds $M[1,3\text{-}(SiMe_3)_2C_3H_3]_2$ (M = Cr, 12-e$^-$;[16] Fe, 14-e$^-$;[20] Co, 15-e$^-$[21,22]); they have no monomeric counterparts with unsubstituted ligands. The neutral monomeric tris(allyl) complexes $Ln[1,3\text{-}(SiMe_3)_2C_3H_3]_3(thf)$ (Ln = Ce, Nd, Tb)[23] and the tetrametallic salt $\{K(thf)_2Sm[1,3\text{-}(SiMe_3)_2C_3H_3]_3\}_2$[24] are likewise without precedent with unsubstituted allyl ligands.

This review is focused on the second type of complex mentioned above; i.e., those (mostly homoleptic) complexes in which the use of sterically bulky allyl ligands has allowed the isolation of complexes with new structural features that are either unknown or substantially different from counterparts with unsubstituted allyl ligands. A brief review of this area was published several years ago, with an emphasis on transition metal complexes;[25] the present microreview updates and expands that review, especially in the areas of main group and lanthanide chemistry. Azaallyl compounds, which have some parallels to those discussed here, have been reviewed elsewhere.[26]

The review is organized along major element families (Groups 1–2, 12–14, and the d- and f-blocks). Synthetic routes that are generally applicable to all the metal families are discussed first.

General Preparative Routes

The most common starting materials for metal complexes containing bulky allyl ligands have been the alkali metal salts of the allyl anions; these are prepared from the lithium allyls, which in turn are generated from the substituted propene and an alkyllithium reagent (Scheme 1).[27] Owing to the pervasive use of the $[1,3\text{-}(SiMe_3)_2C_3H_3]^-$ anion, it will be referred to as "A′" in the rest of this review.

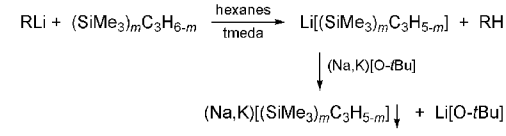

Scheme 1. Synthesis of lithium, sodium and potassium salts of trimethylsilylated allyl anions.

Both mono- and 1,3-dilithiated allylsilanes can be prepared from 1-[(allyldimethylsilyl)methyl]piperidine by treatment with either one or two equivalents of *t*BuLi (Scheme 2). The lithium salts have been structurally characterized.[28]

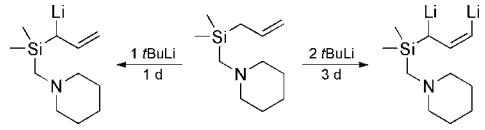

Scheme 2. Mono- and dilithiation of 1-[(allyldimethylsilyl)methyl]-piperidine.

The limited acidity of propene and its substituted derivatives means that direct reaction to form a salt will only occur with the most active metals (Rb, Cs) (Scheme 3).[29]

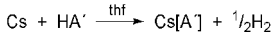

Scheme 3. Synthesis of the cesium salt of the $[A']^-$ anion.

A silyl-bridged bis(allyl)ligand made from the bis(allyl)-silane $Me_2Si(CH_2CHCHSiMe_3)_2$ can be converted into its dilithium or dipotassium salt (i.e., $K_2[3\text{-}(C_3H_3SiMe_3\text{-}1)_2\text{-}SiMe_2]$) (Scheme 4); it has been used in the synthesis of *ansa*-bis(allyl) complexes.[30,31]

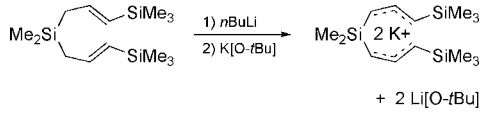

Scheme 4. Synthesis of the dipotassium salt $K_2[3\text{-}(C_3H_3SiMe_3\text{-}1)_2\text{-}SiMe_2]$.

A cyclic allyl variant with sterically bulky groups, the [1,3-bis(trimethylsilyl)-2-cyclohexen-1-yl] anion, has been described. It retains the two trimethylsilyl groups of the $[A']^-$ anion while providing extra shielding with the cyclohexyl group;[32] such protection might be important in mono(π-allyl) metal complexes. The hydrocarbon is synthesized in 3 steps from 3-bromocyclohexene (Scheme 5).

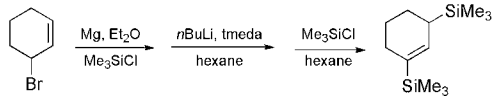

Scheme 5. Synthesis of 1,3-bis(trimethylsilyl)cyclohexene.

A related silyl-bridged bis(cyclohexene) ligand has been used to form *ansa*-bis(allyl) complexes.[32]

Donor-functionalized allyl ligands can provide internal solvation to metal complexes. The reaction of Li[A′] with tetrahydrofurfuryl tosylate produces [4-(tetrahydrofuran-2-yl)but-1-ene-1,3-diyl]bis(trimethylsilane) (Scheme 6); it can subsequently be deprotonated with alkyllithium reagents or $MgBu_2$ to produce new metal complexes.[33]

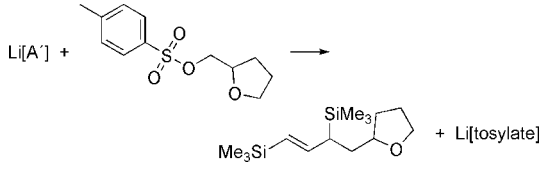

Scheme 6. Synthesis of a thf-functionalized allyl ligand.

Other examples of such functionalized ligands are known. For example, metallation of *N*,*N*-bis(2-methoxyethyl)-2,2-dimethylpent-4-en-1-amine generates a 1:1 equilibrium mixture of two isomeric internally coordinated allyllithium complexes that interconvert on the NMR timescale. Subsequent treatment of the mixture with TMSCl produces trimethylsilyl-substituted allyls which themselves can be lithiated to produce a second pair of interconverting isomers (Scheme 7).[34]

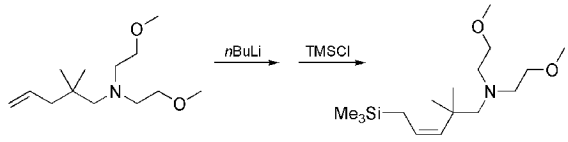

Scheme 7. Synthesis of (*Z*)-*N*,*N*-bis(2-methoxyethyl)-2,2-dimethyl-5-(trimethylsilyl)pent-3-en-1-amine; the (*E*) isomer (not shown) is formed in equal amounts.

Related functionalized allyls ligands have been derived from methoxyethylamino-substituted propenes.[35–37] Other trimethylsilyl-substituted propenes with donor functionalities in the 2-position have been described;[38,39] these have been used in studies of internal solvation on lithium coordination modes.

The terminal substituent in a coordinated allyl ligand can be found in a *syn* or *anti* position; the former conformation places the substituent on the same side of the ligand as the central hydrogen atom; in the *anti* form, the opposite arrangement occurs. To date, π-bound monosubstituted allyl ligands are known only with *syn* orientations, and unless constrained by an *ansa*-bridge, 1,3-disubstituted allyl ligands have *syn*,*syn* configurations in complexes of highly electropositive metals (s- and f-block). Both *syn*,*syn* and *syn*,*anti* arrangements occur in allyl complexes of the d-block transition elements.

Peculiarities of Halide Metathesis Synthesis

Halide metathesis reactions such as that in Scheme 8 are commonly used as a route to bulky allyl metal complexes.

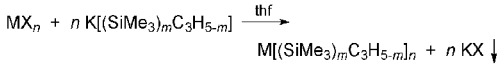

Scheme 8. Metathetical route to allyl complexes.

The use of potassium salts of the allyl anion facilities separation of the alkali halide by-product by filtration of the reaction mixture. Lithium salts, in contrast, are readily solvated by ethers (thf, Et_2O), and can remain mixed with, or even incorporated into, the allyl complexes.

Although synthesis with metathetical methods is typically straightforward, a peculiar difficulty with the use of bulky allyl ligands is that the products of halide-exchange reactions may not reflect the stoichiometry of the reagents. This seems to occur most often with larger metals, especially among the f-elements, although even variations in the metal cation of the allyl starting material can affect the

products isolated. With lanthanide iodides and lithium allyl starting materials, for instance, anionic lanthanates are produced regardless of the lanthanide used (Scheme 9).

$$LnI_3 + n\,K[A'] \xrightarrow{thf} [Li(thf)_4][Ln\{A'\}_3I] + 2\,LiI\downarrow$$
(Ln = Ce, Pr, Nd, Gd, Tb, Ho, Er)

Scheme 9. Metathetical route to lanthanates.

If the potassium derivative of the allyl is used as a starting material, however, neutral species are formed (Scheme 10). The outcomes of some reactions appear to be metal radii dependent.

$$LnI_3 + n\,K[A'] \xrightarrow{thf} Ln[A']_3\ (Ln = Dy, n = 3;\ Ln = Ho, n = 2,3) + n\,KI\downarrow \quad (1)$$

$$LnCl_3 + n\,K[A'] \xrightarrow{thf} Ln[A']_3\ (Ln = Ho, Er, Y, n = 2,3) + n\,KCl\downarrow \quad (2)$$

$$LaCl_3 + n\,K[A'] \xrightarrow{thf} La[A']_2Cl(thf)\ (n = 2,3) + n\,KCl\downarrow \quad (3)$$

Scheme 10. Metathetical route to neutral allyl complexes.

Another example of the lack of strict stoichiometric control is provided by the reaction of two equivalents of K[A′] and $NdI_3(thf)_{3.5}$, which produces a mixture of the expected bis(allyl) complex $Nd[A']_2I(thf)_2$ along with the mono(allyl) compound $Nd[A']I_2(thf)_{1.25}$.[24]

Size effects are clearly operative when it comes to the accommodation of neutral bases in the coordination spheres of the metals. Two sets of reactions have been observed with lanthanide triflates, with a break in composition between Tb and Dy (Scheme 11).

$$Ln[OTf]_3 + 3\,K[A'] \xrightarrow{thf} Ln[A'_3](thf)\ (Ln = Ce, Nd, Tb) + 3\,K[OTf]\downarrow \quad (1)$$

$$Ln[OTf]_3 + 3\,K[A'] \xrightarrow{thf} Ln[A'_3](thf)\ (Ln = Dy, Ho, Er, Tm, Lu, Y) + 3\,K[OTf]\downarrow \quad (2)$$

Scheme 11. Metathetical route to neutral allyl complexes.

With the smaller lanthanides, the coordination sphere is evidently too sterically crowded to incorporate a tetrahydrofuran ligand, although as indicated in Scheme 9, an additional iodide can still be accommodated around a smaller metal.

An unusual twist on this chemistry is that the trimethylsilyl groups in bulky allyl ligands can themselves be sites of reactivity, and traces of water in reagents can initiate unusual transformations.[40] This underscores the need for a high degree of rigor in the purification of reagents and stringent precautions against adventitious admission of air or moisture into reaction systems. Other, more specialized routes to sterically bulky allyl complexes will be described later.

Structures of Compounds from Groups 1–2

(a) The Alkali Metals

Fraenkel and co-workers described the synthesis of lithiated derivatives of the trimethylsilylated propenes, and reported various structural and spectroscopic properties for them.[9–11,34,36–39] The tmeda adduct of Li[A′] is a monomer in the solid state, with slightly asymmetrical π-bonding (e.g., the C–C distances in the allyl ligand differ by 0.041 Å);[9] in solution, however, the molecule appears symmetrical. Lappert has described the structure of the related complex $Li\{1,3\text{-}[Si(tBu)Me_2]_2C_3H_3\}$(tmeda); it is more symmetrical than Li[A′] (e.g., ΔC–C = 0.007 Å), despite the greater bulk of the silyl substituents.[32]

Fraenkel found that the unique trimethylsilyl group at C-3 in the tris(trimethylsilylated) complex $Li[1,1',3\text{-}(SiMe_3)_3C_3H_2]$ was *syn* in solution, and that the barrier to rotation of the allyl groups in thf was 16.8 kcal mol^{-1}.[12] Interestingly, despite the bulk of the ligands, $Li[1,1',3\text{-}(SiMe_3)_3C_3H_2]$ adopts a dimeric structure in the crystal (Figure 2). The two Li atoms are bridged by the allyl ligands in a μ_2-η^1,η^2 manner, with a σ-bonded distance of 2.232(7) Å (Li1–C6′, Li1′–C6). The lithium is centered over the midpoint of the C4–C5 bond, with an average Li–(C4,C5) distance that is indistinguishably different from the σ-bonded length (2.236 Å). The bridging allyls (C4–C6) are only partially delocalized, with a 0.085 Å difference between the single and double bonds.

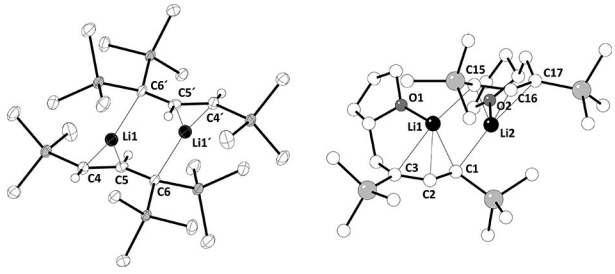

Figure 2. The structures of $\{Li[1,1',3\text{-}(SiMe_3)_3C_3H_2]\}_2$ (left) and bis[μ_2-η^3, η^1-4-(tetrahydrofuran-2-yl)-1,3-bis(trimethylsilyl)but-2-en-1-yl]dilithium (right).

Unsubstituted allyllithium is known to be dimeric in thf solution,[41] and calculations at the DFT level indicate that even the substituted complex $\{Li[C_3\text{-}1,1',3\text{-}(SiH_3)_2H_3](thf)_2\}_2$ would be stable as a dimer.[19] Support for this conclusion is found in a related lithium complex formed from the tetrahydrofurfuryl-substituted derivative of the A′ ligand (Figure 2).[33] The dimeric complex has Li1–O1 and Li2–O2 bond lengths that are indistinguishable at 1.87 Å, and the C–C allyl bonds are slightly more delocalized (Δ = 0.052 Å) than in $\{Li[1,1',3\text{-}(SiMe_3)_3C_3H_2]\}_2$. The lithium atoms have shifted so that they are closest to the center carbon atoms of the allyl ligands [average of Li1–C2 and Li2–C16 bond lengths is 2.196(7) Å] and the distances from the lithium atoms to the "outer" carbon atoms (C3, C17) are now quite long at an average value of 2.48 Å.

The unsolvated 1,3-bis[dimethyl(phenyl)silyl]allyllithium, $Li[1,3\text{-}(SiMe_2Ph)_2C_3H_3]$, forms helical polymeric chains in the solid state (Figure 3).[42] The π-bonded allyl ligands are at an angle of 60–62° from the major chain axes, and the Li–C distances range from 2.16 Å to 2.35 Å. The average distance of 2.26 Å is considerably shorter than the corre-

sponding separation in the polymeric $\{Li[1,3\text{-}Ph_2C_3H_3]\cdot OEt_2\}_\infty$ (2.42 Å),[43] which reflects the presence of the coordinated ethers in the latter complex.

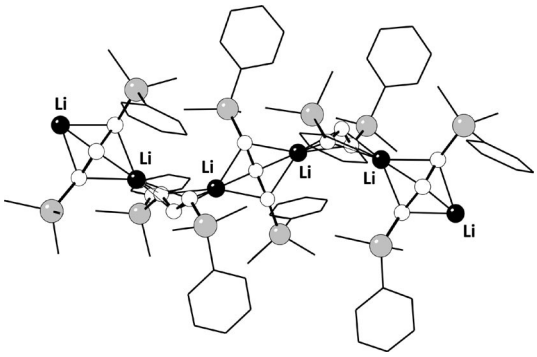

Figure 3. The structure of $\{Li[1,3\text{-}(SiMe_2Ph)_2C_3H_3]\}_\infty$.

Treatment of (1*E*,1′*E*,1″*E*)-3,3′,3″-(methylsilanetriyl)tris(prop-1-ene-3,1-diyl)tris(trimethylsilane) ($MeSiA^{\dagger}_3$) with 3 equiv. of *n*-butyllithium and tmeda produces $Li_3[MeSiA^{\dagger}_3](tmeda)_3$ in 32% isolated yield.[44] The molecular structure of the latter contains a trianionic *ansa*-tris(allyl) ligand with a central tetrahedral Si bound to three allyl moieties and a single methyl group (Figure 4). Each allyl group is in turn bound to a $[Li(tmeda)]^+$ cation. The allyl C–C distances vary over a narrow range of 1.383(7)–1.416(4) Å, which is indicative of a substantial delocalization of the π-electrons in each allyl moiety. As is the case for other solvated lithium allyls, the ^1H NMR spectrum of $Li_3[MeSiA^{\dagger}_3](tmeda)_3$ suggests that it is fluxional in solution.

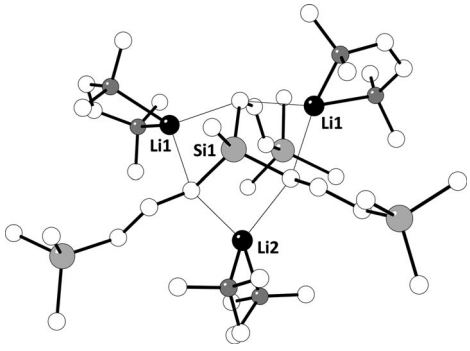

Figure 4. The structure of $Li_3[MeSiA^{\dagger}_3](tmeda)_3$.

Bis(1,3-trimethylsilyl)cyclohexene reacts with *n*-butyllithium and tmeda in hexane at room temperature to yield the lithium derivative (Figure 5).[32] Curiously, although the lithium is well centered over the allyl bond (the difference between Li–C2 and Li–C6 is 0.03 Å), the Li–C1 distance at 2.140(6) Å is much shorter than the average of the Li–C2/Li–C6 distances [2.412(7) Å]; it has been suggested that the lithium–allyl bonding might be considered to be of an η^1-type.

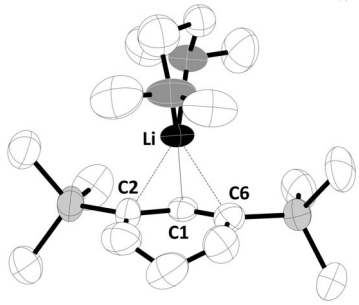

Figure 5. The structure of the lithium derivative of bis(1,3-trimethylsilyl)cyclohexene.

Dilithiation of 1-[(allyldimethylsilyl)methyl]piperidine forms the S_6-symmetric complex hexakis(μ_5-η^3,η^3-1-{dimethyl[(piperidin-1-yl)methyl]silyl}allyl)dodecalithium (Figure 6).[28] In addition to the lithium atoms interacting in a π-type fashion with the allyl ligands (Li–C = 2.16–2.37 Å), a hydrogen at the terminal C3 carbon has been replaced with a lithium atom (Li–C = 2.11 Å). Another close Li···C contact is found at 2.25 Å. DFT calculations on model systems indicate that a substantial amount of the negative potential of the allyl dianion resides near C3, which accounts for its association with multiple lithium centers.

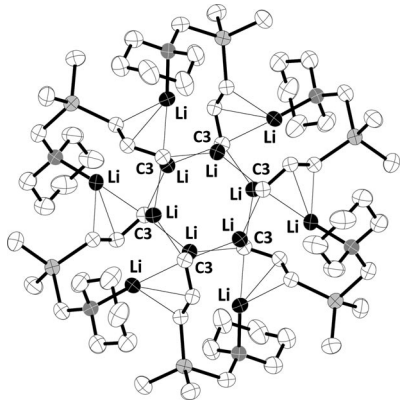

Figure 6. The structure of the dilithium derivative of 1-[(allyldimethylsilyl)methyl]piperidine.

With potassium and the heavier alkali metals, allyl complexes are uniformly found as coordination polymers. The potassium salt of the A′ anion, for example, has been crystallized as DME and thf solvates, $\{K[A'](dme)\}_\infty$[45] and $\{K[(A')(thf)_{3/2}]\}_\infty$,[29] and also as the base-free complex, $\{K[A']\}_\infty$.[19] The tetrahydrofurfuryl-substituted derivative of the A′ anion has been crystallized as its potassium salt,[33] and the dimethylsilyl *ansa*-bis(silylcyclohexenyl)-dipotassium complex $\{K_2[(\eta^3\text{-}C_6H_4SiMe_3\text{-}6)_2SiMe_2]\cdot(thf)_3\}_\infty$ has been isolated as a thf solvate.[32] All five compounds are coordination polymers with potassium ions linked by bridging π-allyl ligands. The $\{K[A']\}_\infty$ polymer takes the form of helical chains running parallel to the *a* axis (Figure 7). The range of K–C distances in $\{K[A']\}_\infty$

(2.87–3.15 Å; Δ = 0.28 Å) is broad enough that the average K–C distance of 3.01 Å is not especially significant, although it is comparable to those for potassium cyclopentadienides (e.g., 2.93 Å to 3.10 Å in $\{K[C_5(SiMe_3)_3H_2]\}_\infty$[46]), indicating the similarly ionic bonding in the complexes.

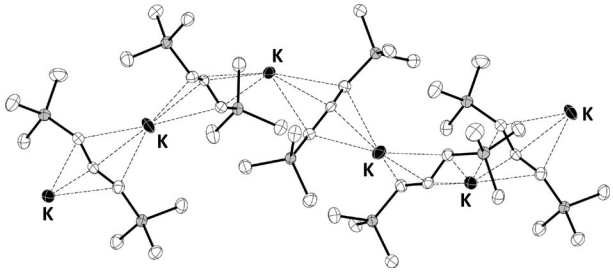

Figure 7. The structure of $\{K[A']\}_\infty$.

The cesium compound $\{Cs[A'](thf)\}_\infty$ forms a strictly linear chain of metal atoms.[29] The immediate environment around the cesium in $\{Cs[A'](thf)\}_\infty$ consists of a thf ligand and two π-bound allyl ligands; there are close intermolecular contacts to methyl groups at 3.67 and 3.95 Å that serve to raise the formal coordination number from 5 to about 7.

(b) The Alkaline-Earth Metals

The alkaline-earth metals display a large range of bonding modes in their allyl complexes. Allyls in magnesium complexes are consistently found to be σ-bonded in the solid state, and η^3-coordination of the allyl ligand to magnesium has been suggested as being disfavored.[33] Nevertheless, the balance between covalent and ionic bonding in allylmagnesium complexes (and corresponding σ- and π-coordination) may be more subtle than indicated by the available solid state data. For example, infrared and ^{13}C NMR spectra indicate that allyl- and [D_2]methallyl-Mg bromides are involved in exchange processes in solution, presumably involving unsymmetrical σ-bonded allylic structures,[47] but the deuterated version of $Mg(C_3H_5)_2$ does not have distinct double bond stretching bands in the IR spectrum, suggesting that delocalized π-type bonding exists in the ligands.[47] Such examples raise the question of just what determines the balance between σ- and π-bonding in allylmagnesium complexes. Structural and computational studies with bulky allyl complexes have provided some insights into this issue.

Prepared by standard metathetical techniques, the colorless complex $Mg[A']_2(thf)_2$ is fluxional in solution; at –45 °C, its ^1H NMR spectrum indicates that the compound possesses σ-bonded A′ ligands.[48] At room temperature and above, however, the spectrum presents an increasingly simplified "π-like" pattern with an apparent triplet, an apparent doublet, and a singlet (for the $SiMe_3$ groups). Similar solution behavior is observed in the GaA'_3 complex (see below),[49] and reflects the presence of equilibrating allylic isomers. In the solid state, each Mg center in $Mg[A']_2(thf)_2$ is surrounded by two σ-coordinated allyl moieties and two thf solvent molecules in a distorted tetrahedral environment. The related compound bis[4-(tetrahydrofuran-2-yl)-1,3-bis(trimethylsilyl)but-2-en-1-yl]dimagnesium demonstrates that internal coordination of thf from donor-functionalized allyl ligands also produces σ-bound coordination.[33]

Under vacuum, the compound $Mg[A']_2(OEt_2)$ is easily desolvated; the resulting yellow, base-free $Mg[A']_2$ complex is fluxional in solution, as evidenced by its ^1H NMR spectrum. In the solid state, $Mg[A']_2$ is a dinuclear species in which the two Mg atoms are coordinated in an irregular fashion (Figure 8).[48] A σ-bound, terminal allyl is present on each magnesium, and two allyl ligands bridge between the metals. The bridging allyls (C14–C16; C24–C26) are of a localized type, and both metals contact them through one relatively short distance of ca. 2.23 Å (Mg1–C26, Mg2–C16). The magnesium to bridging carbon atom distances are considerably longer, and range from 2.435(2) to 2.514(2) Å. The bonding of the magnesium centers to the C14–C16 and C24–C26 carbon atoms is probably of a cation-π nature; similar interactions involving Mg^{2+} have been the subject of computational investigations.[50–53]

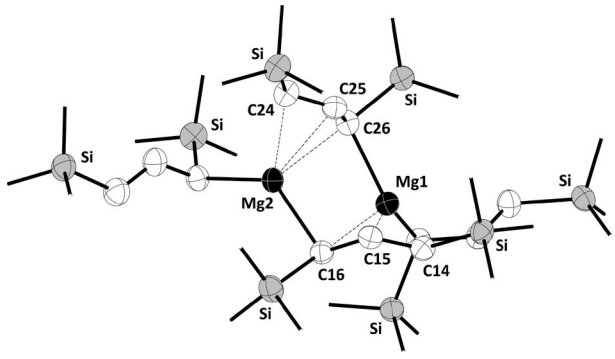

Figure 8. The structure of $\{Mg[A']_2\}_2$. Terminal methyl groups on the silicon atoms have been omitted.

DFT investigations performed on a set of allylmagnesium complexes indicated that the minimum energy structure for $Mg(C_3H_5)_2$ is one with π-bound ligands that are somewhat slipped (Mg–C distances range from 2.23 to 2.33 Å).[48] Calculations indicate that addition of a single thf ligand to $Mg(\pi\text{-}C_3H_5)_2$ results in slippage of one allyl ligand to the classical σ-bonding mode, and addition of a second thf molecule to $Mg(\eta^1\text{-}C_3H_5)(\eta^3\text{-}C_3H_5)\cdot(thf)_2$ causes both allyl ligands to assume σ-bonding modes, like those observed in $Mg[A']_2(thf)_2$ (Figure 9). These results suggest that the near-universal presence of coordinated bases in allylmagnesium species drives the conversion from a delocalized π- to classical σ-bonding.

Like magnesium, the larger metal calcium also forms a colorless complex of the type $M[A']_2(thf)_2$, but the ligands are π-bound. This is suggested by temperature-invariant ^1H NMR spectroscopic data, and confirmed by the solid-state structure. The molecule possesses ligands with delocalized bonding, with the difference between the C–C bonds being less than 0.02 Å (Figure 10).[54]

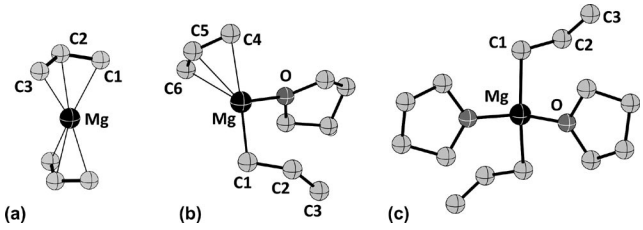

Figure 9. Calculated structures of $Mg(C_3H_5)_2$ (a), $Mg(C_5H_5)_2(thf)$ (b), and $Mg(C_5H_5)_2(thf)_2$ (c). Hydrogen atoms have been omitted for clarity.

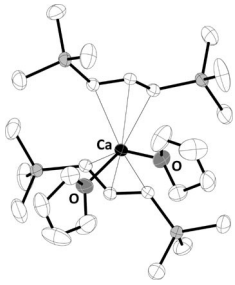

Figure 10. The structure of $Ca[A']_2(thf)_2$.

The allyl ligands are bound in a symmetrical trihapto manner to the metals, with an average Ca–C distance of 2.654(5) Å, respectively. The allyl–M distance is closely similar to that for cyclopentadienyl rings in formally six-coordinate M^{2+} centers [e.g., 2.64(2) Å in $Ca(C_5Me_5)_2$].[55] It is notable that the allyl groups maintain the same metal–ligand separation as do cyclopentadienyl rings, because in transition metal $(C_3R_nH_{5-n})MCp$ complexes, the allyl ligand binds more closely to the metal than does the Cp ring.[56,57]

Structures of Compounds from Groups 12–14

(a) Group 12

When zinc triflate was treated with K[A′], an anionic (triallyl)zincate $K[ZnA'_3]$ was isolated instead of the intended neutral $Zn[A']_2$.[58] Adjustment of the stoichiometry of the reaction (Scheme 12) allowed the synthesis of air- and moisture-sensitive, orange-red crystals of $K[ZnA'_3]$ in high yield. Use of the lithium or sodium salt of the allyl anion produced the analogous yellow lithium and sodium derivatives.

$$Zn(OTf)_2 + 3\ K[A'] \xrightarrow{thf} K[ZnA'_3] + 2\ K[OTf]\downarrow$$

Scheme 12. Synthesis of a potassium tri(allyl)zincate complex.

The lithium compound can also be formed by cation exchange (Scheme 13).

$$K[ZnA'_3] + LiI \xrightarrow{thf} Li[ZnA'_3] + KI\downarrow$$

Scheme 13. Synthesis of a lithium tri(allyl)zincate complex.

It is interesting that the formation of analogous zincates does not occur with the unsubstituted anion; e.g., the parent $Zn(C_3H_5)_2$ is formed even with the use of 2.6 equiv. of $(C_3H_5)MgCl$ per equiv. of $ZnCl_2$.[59]

The $M[ZnA'_3]$ complexes are fluxional in solution, and the NMR chemical shifts are different in C_6D_6, suggesting that the cations remain associated with the zincate anion. In $[D_8]$thf, however, the ^1H NMR chemical shifts are identical, indicating that the alkali metal cations and the zincate anions are now solvent-separated; in particular, the ^7Li NMR spectrum of $Li[ZnA'_3]$ in $[D_8]$thf displays a resonance near that reported for the $[Li(thf)_4]^+$ cation.[60]

Single crystal X-ray structures of $Na[ZnA'_3]$ (Figure 11) and $K[ZnA'_3]$ reveal that the three allyl ligands are bound to the zinc in an arrangement with approximate C_3 symmetry, with the alkali metal cations situated between the double bonds of the allyl ligands. The distances are consistent with noncovalent cation-π interactions. The $K^+\cdots C$(olefin) contacts average 3.205(3) Å and 2.945(3) Å to the carbon atoms β and γ to the zinc atom, respectively. These distances are comparable to the range of $K^+\cdots C$ contacts usually observed with aromatic rings (cf. the 3.12–3.35 Å distances to the neutral arenes in $\{[K(toluene)_2]^+[Mg(N(SiMe_3)_2)_3]^-\}_n$[61]). A closely related type of $K^+\cdots C$(olefin) bonding was observed in a substituted tris(pentadienyl)manganate complex.[62]

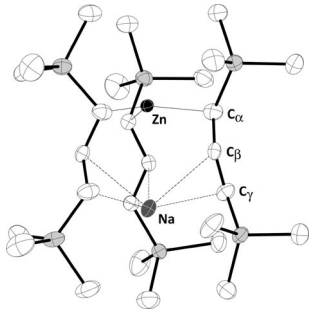

Figure 11. Structure of $Na[ZnA'_3]$; the potassium salt is isostructural. The $Na^+\cdots C$(olefin) contacts average 2.857(3) Å and 2.567(3) Å to the carbon atoms β and γ to the zinc atom, respectively.

The structure of the lithium derivative $Li[ZnA'_3]$ is similar to $Na[ZnA'_3]$ and $K[ZnA'_3]$, but the asymmetry in the metal–carbon distances suggests that some Li–C σ-bonding is involved.[58]

(b) Groups 13, 14

A substituted allyl complex of gallium, pale yellow GaA'_3, has been synthesized from the reaction of K[A′] and $GaCl_3$ in thf and characterized with X-ray crystallography and NMR spectroscopy.[49] It is stable indefinitely under an inert atmosphere and can survive brief (min) exposure to air. In solution at room temperature, the molecule is fluxional and the ligands appear as if symmetrically bound in a π-type fashion e.g., the ^1H NMR resonance for

the $SiMe_3$ groups appears as a sharp singlet, and the central hydrogen atom on the allyl ligands appears as a triplet. A limiting spectrum is not reached even at –75 °C.

In the solid state, the complex displays σ-bound ligands in a trigonal planar arrangement around the metal, with an average Ga–C distance of 1.980(5) Å (Figure 12). The terminal trimethylsilyl groups are *syn* to the central hydrogen atoms of the allyl ligands. The fully localized C–C bonding in the allyl ligands is indicated by the average C=C bond length of 1.329(7) Å and the average C–C bond length of 1.497(6) Å. Density functional theory calculations indicate that the structure found in the solid state, with one allyl ligand antiparallel to the other two, is the lowest in energy, but an alternate arrangement with all three ligands parallel (C_3 symmetry) is less than 3 kcal mol^{-1} higher in energy.

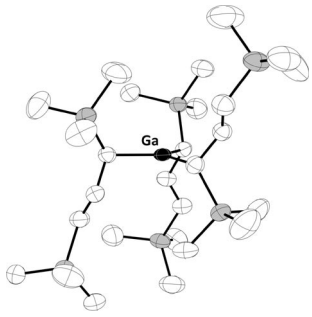

Figure 12. Structure of GaA′$_3$.

Structurally similar to the tris(allyl)zincates noted above is the stannate complex K[SnA′$_3$](thf), synthesized by the salt metathesis of K[A′] and $SnCl_2$ in a 3:1 stoichiometry in thf.[44] X-ray diffraction studies reveal that the Sn resides in a pyramidal environment with C–Sn–C bond angles of 96.7(2)°: this is indicative of the considerable s-character of the tin-centered electron lone-pair. As with the related zincates, the allyl ligands are strongly localized (Δ_{C-C} = 0.16 Å), and the coordination environment for the K^+ ion includes both a thf ligand and the η^2-π-bonds of the allyls [K–C = 3.065(8)–3.164(8) Å].

Unlike the case for the alkali metal zincates and the neutral GaA′$_3$, NMR spectroscopic studies of K[SnA′$_3$](thf) indicate that the σ-bound structure persists in solution, and the ^{1}H NMR spectrum is temperature-independent in the range of 180–298 K. Additionally, ^{119}Sn NMR reveals a single broad resonance at $\delta(^{119}Sn)$ = –132.9 ppm. The static solution behavior of the stannate was attributed to the relative strength of the Sn–C σ-bonds and to the rigidity imparted by the presence of the cation, although the latter is also present in the fluxional zincates.

Structures of d-Block Metal Compounds

Much of the progress with d-block transition metals and sterically bulky allyl ligands has involved the first row metals from Cr to Ni. In contrast, with the exception of the early (Groups 4 and 5) metals, complexes of the second and third row transition elements have yet to be isolated.

(a) Group 4 Complexes

Reaction of $TiCl_4$ or $ZrCl_4$ with two equivalents of Li[1,3-(Si(*t*Bu)Me_2)$_2$$C_3H_3$](tmeda) generates the trivalent complexes [1,3-(Si(*t*Bu)Me_2)$_2$$C_3H_3$]$_2$(Ti,Zr)(μ-Cl)$_2$Li(tmeda), along with the coupled dimer of the allyl ligand.[13] Some of the allyl anion serves as the reducing agent, which reduces the yield of the metal complex below 50%. In the solid-state structures of both compounds, the allyl ligands are slightly slipped to one side of the metal, suggesting a distortion toward a σ,π-(η^3) bonding arrangement. In the titanium complex (Figure 13), for example, the difference between the Ti–$C_{terminal}$ distances is ca. 0.2 Å. Both the titanium and zirconium complexes can be oxidized to form neutral tetravalent species [1,3-(Si(*t*Bu)Me_2)$_2$$C_3H_3$]$_2(Ti,Zr)Cl_2$, which display $\eta^3 \rightleftarrows \eta^1$ allyl ligand fluxionality on the ^{1}H NMR timescale.

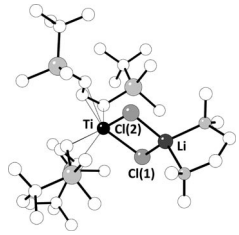

Figure 13. The structure of [1,3-(Si(*t*Bu)Me_2)$_2$$C_3H_3$]$_2$Ti(μ-Cl)$_2$Li(tmeda).

Hafnium tetrachloride reacts with [Li(tmeda)]$_2$[3-($C_3H_3SiMe_3$-1)$_2$$SiMe_2$] to form the *ansa*-bis(allyl) complex Hf[3-($C_3H_3SiMe_3$-1)$_2$$SiMe_2$]$_2$, and zirconium tetrachloride reacts with the dipotassium derivative of the same allyl anion to produce Zr[3-($C_3H_3SiMe_3$-1)$_2$$SiMe_2$]$_2$.[30] The latter molecule lies on a crystallographic twofold axis, with the allyl ligands binding in a η^3-chelating manner; the Zr–C distances range from 2.46 to 2.59 Å (Figure 14).

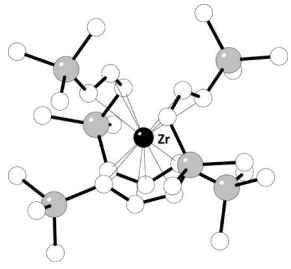

Figure 14. The structure of Zr[3-($C_3H_3SiMe_3$-1)$_2$$SiMe_2$]$_2$.

(b) Group 5 Complexes

The tin allyl (Me_3Si)CH=CHCH($SiMe_3$)($SnMe_3$)(SnA′Me_3) has been synthesized in high yield via reaction of K[A′] and Me_3SnCl.[44] The resulting air-stable colorless oil was used in the dehalostannylation of $TaCl_5$ to afford TaA′Cl_4 as red microcrystals. The ^{1}H NMR spectrum, which contains an apparent singlet, doublet, and triplet, is indicative of a π-bound allyl. However, because X-ray quality crystals could not be obtained, the product was allowed

to react with tmeda, and surprisingly afforded the tantalum alkylidene complex $Me_3SiCH{=}CHC(SiMe_3){=}TaCl_3$(tmeda) (Figure 15). The formation of the alkylidene was attributed to dehydrochlorination by tmeda in concert with the formation of tmeda·HCl.

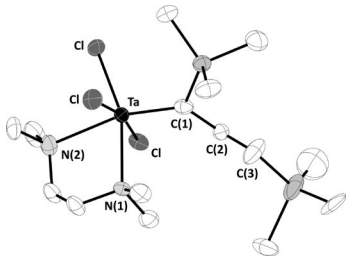

Figure 15. The structure of $Me_3SiCH{=}CHC(SiMe_3){=}TaCl_3$-(tmeda).

The tantalum center is confined to a distorted octahedral environment. Because it is bound *trans* to both a Cl ligand and the alkylidene, the tmeda is unsymmetrically bound: the Ta–N(2) distance that is *trans* to the alkylidene is significantly longer [2.507(6) Å] than the Ta–N(1) distance *trans* to the Cl [2.375(5) Å]. The Ta–C(1) bond [1.953(7) Å] is consistent with other bonds of this type. Additionally, the difference between the C(1)–C(2) and C(2)–C(3) distances (0.17 Å) is indicative of a significant localization of π-electrons, consistent with the presence of a vinyl alkylidene.

(c) Group 6 Complexes

Divalent chromium compounds demonstrate how bulky allyl ligands can be used to tune molecular structures. The unsubstituted allyl anion forms a diamagnetic compound with chromium that has been structurally characterized as a quadruply bonded dimer, $\{Cr(C_3H_5)_2\}_2$.[63] Interestingly, use of the monosubstituted ligand $[1\text{-}(SiMe_3)C_3H_4]^-$ does not impose major structural changes on the basic $\{Cr(allyl')_2\}_2$ framework; the structure of $\{Cr[1\text{-}(SiMe_3)\text{-}C_3H_4]_2\}_2$ is closely similar to that of the parent complex, including the length of the Cr–Cr bond (1.9784(7) Å and 1.97 Å, respectively) (Figure 16).[16]

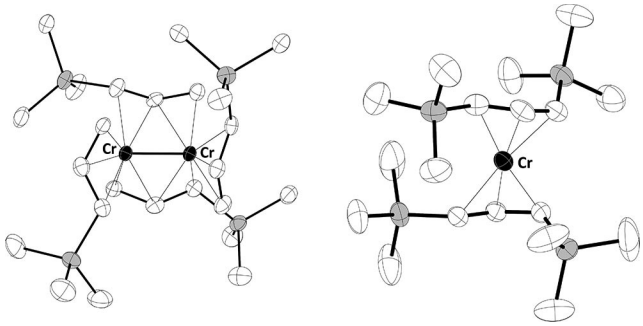

Figure 16. The structures of $\{Cr[1\text{-}(SiMe_3)C_3H_4]_2\}_2$ (left) and CrA'_2. In $\{Cr[1\text{-}(SiMe_3)C_3H_4]_2\}_2$, $Cr–C_{(terminal)}$ = 2.19(1)–2.303(5) Å, $Cr–C_{(bridge)}$ = 2.123(6)–2.164(9) Å. In CrA'_2, Cr–C = 2.193(2)–2.257(2) Å.

With the bulkier $[A']^-$ anion, a monomeric high-spin 12-e$^-$ complex is generated; the staggered ligands display *syn*,*anti* trimethylsilyl groups (Figure 16). Despite its electron deficiency, CrA'_2 displays remarkable thermal stability, e.g., it is stable in boiling toluene (110 °C) and sublimes at 65 °C and 10^{-2} Torr. Calculations on the model compound $Cr(C_3H_5)_2$ have been used to rationalize the electronic structure of CrA'_2.[16] The relatively close spacing (<0.3 eV) of the four frontier orbitals of $Cr(C_3H_5)_2$ is responsible for its predicted high-spin state, and the large HOMO–LUMO gap of 5.25 eV is consistent with a thermodynamically stable compound. CrA'_2 is also high-spin and stable, suggesting that the trimethylsilyl groups do not affect the spacing of the energy levels appreciably.

Increasing the bulk of the allyl ligand further does not materially change the structure of the resulting complex. The complex $Cr[1,1',3\text{-}(SiMe_3)_3C_3H_2]_2$ crystallizes from hexanes as a monomer with crystallographically imposed inversion symmetry.[16] The allyl ligands in the compound are arranged about the metal in a staggered configuration, as in CrA'_2.

The progressive limiting of reactivity with the increase in steric bulk is apparent in the reaction of the complexes with phosphanes. CrA'_2 does not react with PPh_3 at atmospheric pressure and ambient temperatures, but PMe_3 will form a 1:1 adduct, $CrA'_2(PMe_3)$. However, $Cr[1,1',3\text{-}(SiMe_3)_3\text{-}C_3H_2]_2$ fails to react even with PMe_3, and can in fact survive brief (minutes) exposure to air without substantial decomposition.

(d) Group 7 Complexes

When three equivalents of Li[A′] are allowed to react with $MnCl_2$ in thf, the red-brown tris(allyl) manganate $[Li(thf)_4][MnA'_3]$ is isolated.[64] The anion contains both an η^3-bonded and two η^1-bonded allyl ligands (Figure 17). The two σ-bonded allyl groups display nearly identical Mn–C lengths averaging, 2.186(6) Å, whereas the distance to the π-bonded allyl is considerably longer, at 2.348(3)–2.470(4) Å. Despite the spread in the latter values, the difference between the C–C bonds is only 0.01 Å, indicating complete π-electron delocalization. Magnetic measurements on the complex indicate that an incomplete spin state change occurs between the S = 1/2 and S = 5/2 states of Mn^{II} in the temperature range 5–300 K, similar to the behavior of some manganocenes.[65,66] Computational studies of the $[MnA'_3]^-$ anion and the parent unsubstituted com-

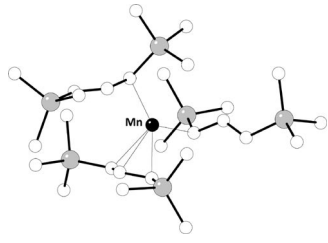

Figure 17. The structure of the anion of $[Li(thf)_4][MnA'_3]$.

plex suggest that the trimethylsilyl substituents have little effect on the geometry; this is true whether the complex was optimized with the $S = 3/2$ or $S = 5/2$ spin state. The η^1-bonded ligands were found to display more covalent character than the η^3-bonded allyls.[66]

(e) Complexes of Groups 8–10

The divalent first-row MA'_2 compounds were among the first to illustrate the remarkable stabilizing ability of bulky allyl ligands.[17,20–22] Halide metathetical routes can be used to synthesize all three MA'_2 compounds (M = Fe, Co, Ni), although halide exchange can be problematic for nickel (see below), and for iron an additional route starting from a lithium ferrate complex has been described (Scheme 14).[67]

$$[Li(tmeda)]_2[Fe(C_2H_4)_4] + 2\ C_3(SiMe_3)_2H_3Br \xrightarrow[-78\ °C]{thf} + FeA'_2 + 2\ LiBr(tmeda) + 4\ C_2H_4$$

Scheme 14. Synthesis of FeA′2 from a ferrate complex.

The complexes are soluble in ethers and both aromatic and aliphatic hydrocarbons. The iron and cobalt compounds are highly air-sensitive, but are indefinitely stable under a nitrogen atmosphere. The nickel compound is stable in water for several hours and in air for several days. The thermal stability conferred on the complexes by the trimethylsilyl substituents is such that all have melting points above 50 °C, and can be sublimed under vacuum without decomposition. The Fe, Co, and Ni complexes have magnetic susceptibilities corresponding to 2, 1, and 0 unpaired electrons, respectively.

A staggered MA'_2 arrangement with *syn*,*anti* trimethylsilyl groups is found for the cobalt and nickel analogues,[17,21,22] although the nickel complex is also found with eclipsed allyl ligands and the iron complex exclusively so. The reason for the difference is unclear. Isolation of the iron and cobalt species is particularly noteworthy, as there are no unsubstituted $M(C_3H_5)_2$ analogues known.

The effect of bulky ligands can be observed in the similarity of some core parameters of the MA'_2 complexes (Table 1). Longer M–C bonds are observed for the Cr species, owing to its extreme electron deficiency, but the Fe, Co, and Ni bond lengths are similar. The interplanar C_3 angle is also moderated by the trimethylsilyl groups; staggered molecules are the least congested with only slightly inclined ligands (angles close to zero); the eclipsed structures are forced back to angles exceeding 50°.

By far the most work on the first row allyl complexes has been done with the nickel species NiA'_2. Its synthesis from metal halides proved non-routine, in that the reaction of K[A′] with $NiCl_2$, $NiBr_2$, and NiI_2 leads to the formation of the trimethylsilylated hexadiene $[(SiMe_3)_2C_3H_3]_2$. In contrast, use of $Ni(acac)_2$[44] or the more soluble halide $NiBr_2(dme)$[17] leads to the isolation of the yellow-orange product in high yields. Electrochemical investigations of NiA'_2 revealed only an irreversible, one-electron oxidation in both thf and dichloromethane.

Table 1. Metal–carbon bond lengths [Å] and interplanar ligand angles [°] in MA'_2 complexes.

Compound	Formal e^- count	M–C distance	Angle between allyl planes
CrA'_2[a]	12	2.195(2)–2.257(2)	10.4
$Cr[1,1',3\text{-}(SiMe_3)_3C_3H_2]_2$[a]	12	2.223(5)–2.319(5)	10.4
FeA'_2[b]	14	1.998(2)–2.084(2)	52.7
CoA'_2[a]	15	1.996(3)–2.096(3)	4.7
NiA'_2[b]	16	1.944(3)–2.037(3)	56.7
NiA'_2[a]	16	1.980(1)–2.031(1)	4.4

[a] Staggered. [b] Eclipsed.

NMR spectra of NiA'_2 indicate that eclipsed (*cis*) and staggered (*trans*) forms are present in solution. The relative amounts of the eclipsed and staggered conformers change with temperature for both $Ni(C_3H_5)_2$ and NiA'_2, although not in the same way. For $Ni(C_3H_5)_2$, the staggered form is always dominant, although at higher temperatures more of the eclipsed form is present. The two conformers remain interconvertible at all temperatures.[68] In contrast, the reaction to form NiA'_2 generates a mixture of *cis*-NiA'_2 and *trans*-NiA'_2 in varying proportions, but the eclipsed *cis*-NiA'_2 is dominant when the reaction is conducted at –78 °C. If the reaction to form NiA'_2 is conducted at room temperature, *trans*-NiA'_2 is found to be predominant, with a *cis*-NiA'_2: *trans*-NiA'_2 ratio of 2:3. Irreversible conversion of *cis*-NiA'_2 to *trans*-NiA'_2 occurs on heating a sample to 380 K.

It is noteworthy that only the *trans* form of $Ni(C_3H_5)_2$ is known in the solid state, whereas both *cis*- and *trans*-NiA'_2 can be isolated as physically separable crystals, additional evidence that the two forms do not interconvert at room temperature. The Ni–C bonds in *cis*-NiA'_2 and *trans*-NiA'_2 are similar, although their interplanar C_3 angles are noticeably different (Table 1 and Figure 18).

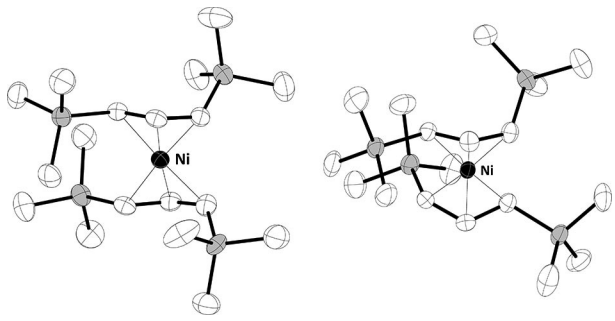

Figure 18. Structures of *trans*-NiA'_2 (left) and *cis*-NiA'_2 (right).

The crystal structures of $Ni(C_3H_5)_2$ and *trans*-NiA'_2 are remarkably similar in the core features of their metal–ligand geometries. The nickel–carbon bond lengths are within 0.04 Å of each other, and the angles between the C_3 planes differ by less than 5°, even though DFT calculations suggest that the potential energy surface for the interplanar angle is nearly flat, and presumably easily changeable by bulky ligand substitutents.[17]

The mono(allyl)nickel species A′NiBr can be formed by the reaction of bis(trimethylsilyl)allyl bromide with $Ni(COD)_2$ (Scheme 15), or by the direct reaction of NiA'_2 with elemental bromine in benzene at 0 °C (Scheme 16).

$$C_3(SiMe_3)_2H_3Br + Ni(COD)_2 \longrightarrow \textit{syn,syn}\text{-A′NiBr} + 2\,COD$$

Scheme 15. Synthetic route to *syn*,*syn*-A′NiBr.

$$NiA'_2 + Br_2 \xrightarrow{0\,^\circ C} \textit{syn,anti}\text{-A′NiBr} + C_3(SiMe_3)_2H_3Br$$

Scheme 16. Synthetic route to *syn*,*anti*-A′NiBr.

The red-purple A′NiBr is an air- and moisture-sensitive solid. Its NMR spectrum indicates that the trimethylsilyl groups are equivalent, and thus in a *syn*,*syn* arrangement when prepared from $Ni(COD)_2$, but the product derived from NiA'_2 has inequivalent trimethylsilyl groups, hence preserving the arrangement found in the parent complex. Unlike the unsubstituted complex $(C_3H_5)NiBr$, which rearranges in donor solvents via a Schlenk equilibrium into $Ni(C_3H_5)_2$ and $NiBr_2$,[69] the trimethylsilylated version is stable to rearrangement under such conditions.

The A′NiBr complex crystallizes from hexanes as a bromide-bridged dimer. The molecule lies on a crystallographic twofold axis, and only half of the molecule is unique (Figure 19). The Ni–C bond lengths range from 1.978(6) to 2.062(7) Å, and the Ni–Br1 and Ni–Br2 bond lengths are identical within error [2.362(10) and 2.365(1) Å].

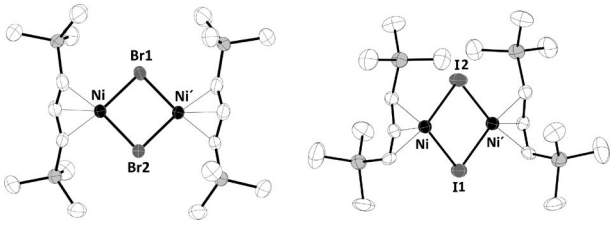

Figure 19. Structures of $\{A'NiBr\}_2$ (left: bromine Br2 lies on a twofold axis, Br1 lies slightly off the axis) and of the eclipsed form of $\{A'NiI\}_2$ (right: a staggered version is also found in the same unit cell).

Iodine reacts smoothly with NiA'_2 in hexanes to yield a red-purple solid that can be recrystallized from hexanes as dark red blocks (Scheme 17).

$$NiA'_2 + I_2 \longrightarrow \textit{syn, anti}\text{-A′NiI} + C_3(SiMe_3)_2H_3I$$

Scheme 17. Synthesis of A′NiI.

The NMR spectroscopic data are complex, as not only are inequivalent trimethylsilyl groups evident, indicative of a *syn*,*anti* arrangement, but two diastereomers are also present. These likely correspond to the staggered and eclipsed conformers found in the solid state (Figure 19). In thf, A′NiI is stable to rearrangement in donor solvents.

Structures of f-Block Metal Compounds

Like the metals of the heavier s-block, elements of the f-block (lanthanides and actinides, and conventionally also scandium and yttrium) have large radii (> 0.90 Å) and are highly electropositive. The range of oxidation states displayed in many of their organometallic compounds (2–4) gives rise to a complex variety of structural types.

(a) Neutral $M(allyl')_n \cdot L$ Complexes

Interestingly, the prototypal structure $M(C_3H_5)_3$ is unknown in structurally authenticated lanthanide complexes; such complexes are invariably crystallized as oligomers or coordination polymers with bridging donor ligands.[70] The additional steric demand of bulky allyl ligands can prevent such oligomerization; an example is the tris(η^3-allyl) thulium complex, $Tm[A']_3$ (Figure 20).[71] The molecule is disordered over a threefold axis, with the ligands arranged around the metal center such that one allyl ligand is oriented roughly *anti*-parallel to the other two (Figure 20). The trimethylsilyl groups are in a *syn*,*syn* configuration, as is found with other trimethylsilyl-substituted allyl lanthanide complexes.[23,24,45,72] A related disordered structure was found for $Y[A']_3$,[73] and similar structures probably exist for $Ln[A']_3$ (Ln = Dy, Ho, Er, Lu).[71]

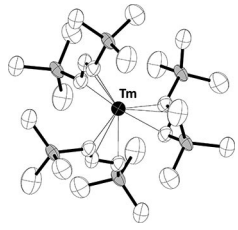

Figure 20. The structure of $Tm[A']_3$. Tm–C bond lengths range from 2.326(2) to 2.606(2) Å, with an average of 2.53(1) Å.

Monomeric structures are also found for the homoleptic tetrakis(allyl)thorium complexes $Th[(SiMe_3)_nC_3H_{5-n}]_4$ (n = 1,2).[18] The thorium complexes contain four *syn* or *syn*,*syn* η^3-ligands (Figure 21); in the case of $Th[1\text{-}(SiMe_3)C_3H_4]_4$, they are in a configuration with approximate S_4 symmetry.[18]

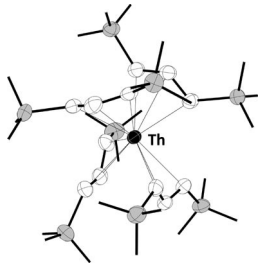

Figure 21. The structure of ThA'_4. Terminal methyl groups on the silicon atoms have been omitted. Th–C bond lengths range from 2.617(5) to 2.892(5) Å, with an average of 2.77(3) Å.

The $Th[(SiMe_3)_nC_3H_{5-n}]_4$ compounds are stable up to 90 °C (n = 1) or 124 °C (n = 2) under an inert atmosphere. The stability of these complexes contrasts strongly with $Th(C_3H_5)_4$, which decomposes at 0 °C.[3] Both molecules are fluxional on the ^{1}H NMR timescale, and $\eta^3 \rightleftarrows \eta^1$ ligand rearrangements are involved in the interchange of their allylic protons.

An unusual transformation of a neutral tris(allyl) species is observed with the holmium complex $Ho[A']_3$.[40] The unsolvated complex can be produced from rigorously anhydrous $HoCl_3$ and K[A′] according to Scheme 11. If the $HoCl_3$ used is partially hydrated (ca. 3% water), $Ho[A']_3$ is still produced if the reaction time is relatively short (<4 h), but at longer times a series of transformations is induced. After 15 h, a dinuclear yellow-orange complex, $[A']Ho(\mu\text{-}L)_2Ho[A']$; [L = $CH_2SiMe_2(CH)_3(SiMe_3)$], can be isolated in good yield. One η^3-coordinated allyl ligand is bound to each metal, but hydrogen abstraction from a trimethylsilyl group has occurred on a second allyl ligand associated with each metal center, forming dimethylsilylene units that bridge the holmium atoms. The bridging carbon atoms are nearly symmetrically positioned between the holmium centers (Figure 22).

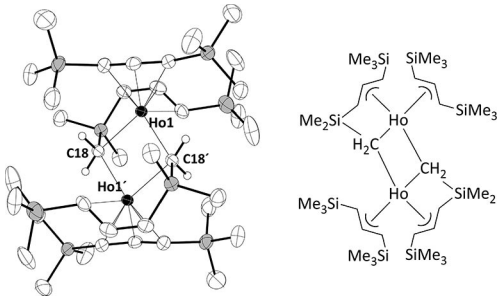

Figure 22. Left: the structure of $[A']Ho(\mu\text{-}L)_2Ho[A']$. Hydrogen atoms not part of the dimethylsilylene bridges have been omitted. Selected bond lengths [Å]: Ho1–C18, 2.478(4); Ho1′–C18, 2.512(4). Right: schematic view of the same.

When the reaction with hydrated $HoCl_3$ is allowed to continue for more than 20 h before workup, a second yellow-orange dinuclear product can be isolated. In addition to two dimethylsilylene bridges, the metal centers are joined with a μ-η^1,η^3-allylidene ligand (Figure 21). Both crystallographic and computational studies provide evidence for delocalized bonding in the allylidene fragment (Figure 23).

The detailed mechanisms of these transformations are not known, although there are parallels in transition metal chemistry, and C–H activation of trimethylsilyl groups is known in cyclopentadienyl compounds of the early transition metals.[74–76] A possible reaction sequence involving the initial, rapid formation of the neutral $Ho[A']_3$ complex followed by a series of water-enabled protonation and hydrogen abstraction steps has been proposed.[40] It is clear that trimethylsilyl groups on allyl ligands cannot always be assumed to be completely unreactive.

Neutral, solvated tris(allyl) species $Ln[A']_3(thf)$ (Ln = Ce, Nd, Tb) can be produced according to Scheme 13.[23] The neodymium complex (Figure 24) has three η^3-coordinated

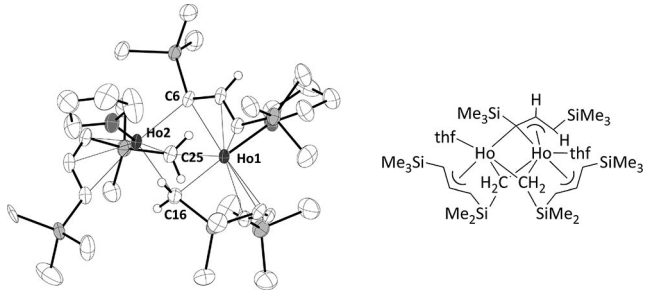

Figure 23. Left: the structure of a holmium allylidene complex. Hydrogen atoms not part of the bridging ligands have been omitted. Selected bond lengths [Å]: Ho1–C6, 2.500(5); Ho2–C6, 2.422(5); Ho1–C16, 2.570(5); Ho2–C16, 2.517(5); Ho1–C25, 2.629(5); Ho2–C25, 2.519(5). Right: schematic view of the same.

allyl ligands, with an approximate threefold axis through the Nd–O bond [2.609(3) Å]; Nd–C distances range from 2.64 to 2.78 Å. The cerium and terbium complexes are isostructural. The thf ligand is not removed on reaction with Me_3SiI or on sublimation, a reflection of the strength of the Ln–O interaction.

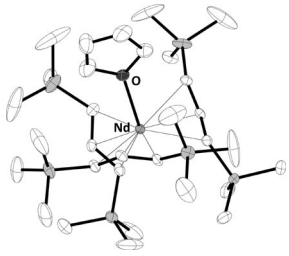

Figure 24. The structure of $Nd[A']_3(thf)$.

Consistent with the stability of the divalent oxidation states of ytterbium and europium, the triflates of Yb^{III} and Eu^{III} are reduced by the A′ anion, leading to Ln^{II} species (Scheme 18).[45] The same compounds can be made in higher yield by starting with Yb^{II} and Eu^{II} triflates directly.

$$Ln(OTf)_3 + 3\,K[A'] \xrightarrow{thf} Ln[A']_2(thf)_2 + {}^1/_2(A'H)_2 + 3\,K[OTf]\downarrow$$

Scheme 18. Synthesis of divalent lanthanide allyl complexes by reduction.

On reaction with two equivalents of the appropriately substituted allyl anions, the divalent halide $SmI_2(thf)_2$ forms the neutral bis(allyl)complexes $Sm[A']_2(thf)_2$ and $Sm[1,3\text{-}Ph_2C_3H_3]_2(thf)_2$.[77]

(b) Anionic $[M(allyl')_n{\cdot}L]^-$ Complexes

Lanthanates of the general formula $[Li(thf)_4][Ln\{A'\}_3I]$ have been produced according to Scheme 9, and their structures confirmed with X-ray analysis of the Ce, Er and Tb species.[23] The erbium derivative is typical for the set, with Er–I = 2.979(8) Å, and Er–C distances ranging from 2.61 to 2.64 Å (Figure 25).

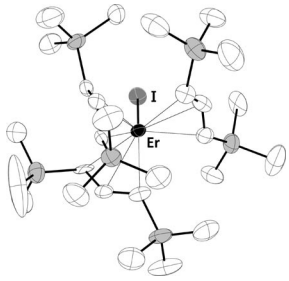

Figure 25. The structure of the anion of $[Li(thf)_4][Er\{A'\}_3I]$.

(c) Heterometallic Complexes

Reaction of $ScCl_3(thf)_3$ with two equivalents of Li[A′] in thf might be expected to produce the allyl halide complex, $Sc[A']_2Cl$. As occasionally happens with the use of lithium-based reagents in thf, the by-product $LiCl(thf)_n$ is trapped and incorporated into the product, yielding the heterometallic bis(π-allyl) complex $[A']_2Sc(\mu\text{-}Cl)_2Li(thf)_2$.[78] The Sc–C distances range from 2.31–2.46 Å, and the Sc–Cl distances are nearly identical at 2.44 Å (Figure 26).

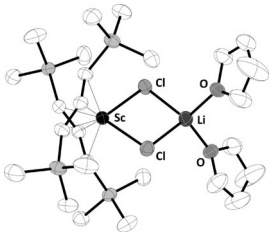

Figure 26. The structure of $[A']_2Sc(\mu\text{-}Cl)_2Li(thf)_2$.

The reaction of three equivalents of K[A′] with $SmI_2(thf)_2$ results in a lanthanate with the empirical formula $K(thf)_2[Sm\{A'\}_3]$. In the solid state, the compound appears as the tetrametallic salt $\{K(thf)_2Sm[A']_3\}_2$ (Figure 27).[24] The samarium and potassium ions are linked by four η^3-allyl ligands, and the potassium ions, which are in three separate coordination environments, display both π- and agostic interactions with the allyl ligands. There is evidence from ^1H NMR spectra that the compound persists as a tetramer in solution.

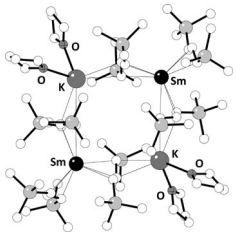

Figure 27. The structure of $\{K(thf)_2Sm[A']_3\}_2$.

Various lanthanide halides ($ScCl_3$, YCl_3, $LaCl_3$, NdI_3) react with $K_2[3\text{-}(C_3H_3SiMe_3\text{-}1)_2SiMe_2]$ to form heterometallic *ansa*-bis(allyl) complexes. The lanthanum derivative has been structurally authenticated as a coordination polymer, in which allyl anions interleave between lanthanum and potassium ions; the latter display K···MeSi contacts of 2.79(3) and 2.96(4) Å (Figure 28).[31]

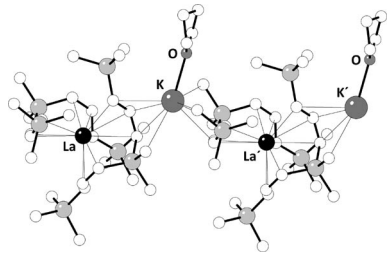

Figure 28. The structure of $\{La(\eta^3\text{-}C_3H_3SiMe_3)_2SiMe_2\}_2\{\mu\text{-}K(thf)\}_\infty$.

Curiously, when the divalent starting material $SmI_2(thf)_2$ reacts with a $Li_2[3\text{-}(C_3H_3SiMe_3\text{-}1)_2SiMe_2]$/KO-*t*Bu mixture in light petroleum/Et_2O, the *ansa*-bridged *trivalent* Sm^{III} complex $[Li(OEt_2)_4][Sm\{(\eta^3\text{-}C_3H_3SiMe_3)_2SiMe_2\}_2]$ precipitates in low yield.[31] Formed by an obscure redox reaction, the anion lies on a crystallographic twofold axis, with the allyl ligands binding in a η^3-chelating manner (Figure 29). Sm–C distances vary from 2.70–2.74 Å, and the trimethylsilyl substituents are in a *syn*,*anti* configuration.

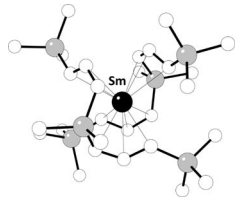

Figure 29. The structure of the anion of $[Li(OEt_2)_4][Sm\{(\eta^3\text{-}C_3H_3SiMe_3)_2SiMe_2\}_2]$.

A test of the resemblance of substituted diallylytterbium complexes to decamethylytterbocene [i.e., $Yb(C_5Me_5)_2$] led to an exploration of the electronic interactions of bulky allyl ytterbium complexes with terpyridyl ligands. Adducts of ytterbocene with *N*-heterocyclic ligands display a stable electronic configuration derived from a spontaneous electron transfer from a diamagnetic Yb^{II} f^{14} metal center to the lowest unoccupied molecular orbital (LUMO) on the *N*-heterocyclic ligand ($f^{14}\text{-}\pi^{*0} \rightarrow f^{13}\text{-}\pi^{*1}$).[79–81] A variety of diallylytterbium complexes with the allyl ligands [1-(SiMe$_3$)$C_3H_4]^-$, $[A']^-$, and the asymmetric allyl ligand [1-(SiPh$_3$)-3-(SiMe$_3$)$C_3H_3]^-$ were synthesized by mixing the ytterbium complex with the *N*-heterocycles in thf at –30 °C. X-ray quality crystals of $Yb[A']_2(tpy)$ (tpy = terpyridine) provided the structure of the adduct (Figure 30). The allyl ligands are π-bound to the ytterbium center with Yb–C bond lengths ranging from 2.52(2) to 2.62(2) Å; these distances are consistent with allyl ligands bound to a Yb^{III} center, evidence that electron transfer from the Yb^{II} center to the tpy ligand has occurred.

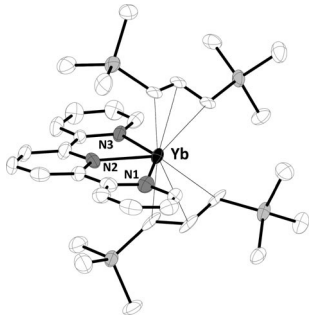

Figure 30. The structure of Yb[A′]$_2$(tpy). The tpy ligand is η^3-bound to the metal center with Yb–N bond lengths from 2.27(2) to 2.39(2) Å.

Variable-temperature magnetic susceptibility measurements on Yb[A′]$_2$(tpy) are also in harmony with the valence tautomer model proposed for Yb(C$_5$Me$_5$)$_2$(tpy). Corroborating evidence for the model was found in the C≡N stretching frequencies of the nitrile-substituted terpyridine adducts (e.g., the C≡N stretching frequency of Yb[A′]$_2$(tpy(CN)$_2$) (2125 cm^{-1}) is within 5 cm^{-1} of that for the [tpy(CN)$_2$]$^-$ anion, a result of a high degree of electron transfer from the metal center to the terpyridine ligand.)

Metal–Ligand Distances in Bulky Allyl Lanthanide Complexes

Analysis of the M–C bond lengths in various monomeric divalent and trivalent allyl complexes has been used to identify an allyl "radius" from the difference between the metal–carbon distance and the metal radius.[71] This approach is similar to one previously used with cyclopentadienyl complexes,[82–84] and the constant value of the radius is a measure of the ionicity of the M–L bonding (i.e., $D_{M-L} = r_+ + r_-$).

Despite the geometrically irregular shape of the substituted allyl anion, metal–ligand distances for the trivalent compounds appear to be reasonably predictable based on metal radius and oxidation state. With the exception of Tm[A′]$_3$, the range in allyl radii is very narrow (1.675 to 1.70 Å). The slightly smaller ligand radius for Tm[A′]$_3$ (1.65 Å) is possibly an artifact of the disorder in the crystal structure.

There is somewhat greater spread in the distances in divalent compounds; in particular, the dissimilarity in the calcium and ytterbium complexes' M–C bond lengths is unexpected (Table 2).[45] Because the ionic radii of calcium and ytterbium differ only slightly (Ca^{2+}, 1.00 Å; Yb^{2+}, 1.02 Å for CN 6),[85] bond lengths and angles of the ligands in their respective complexes are usually similar.[86] An argument has been made that the longer Yb–C bonds reflect bond weakening arising from the filled f^{14} shell of the Yb^{2+} ion.[45]

Table 2. Bond lengths for monomeric divalent lanthanide and alkaline-earth allyl complexes. All bond lengths and radii are in Å.

Complex	Radius	M–C	M–C (av.)	R_{M-C}[a]
Eu[A′]$_2$(thf)$_2$	1.17 (CN 6)	2.762(14)–2.789(14)	2.77(2)	1.60
Sm[A′]$_2$(thf)$_2$	1.17 (CN 6)	2.765(6)–2.796(6)	2.78(1)	1.61
[Sm{A′}$_3$]$^-$	1.17 (CN 6)	2.743(5)–2.895(5)	2.84(1)	1.67
Yb[A′]$_2$(thf)$_2$	1.02 (CN 6)	2.729(9)–2.754(9)	2.74(1)	1.72
Ca[A′]$_2$(thf)$_2$	1.00 (CN 6)	2.648(3)–2.662(3)	2.654(5)	1.654

[a] R_{M-C} is the allyl anion "radius", defined from metal–carbon distances.

Reactions and Applications

Owing to the relative newness of the area, extensive studies of the reactions of complexes with bulky allyl ligands have yet to be made. In addition to some of the unusual preparative reactions already noted, various multistep but non-catalytic reactions have been reported. For example, the tris(allyl) complex Y{1-[Si(*t*Bu)Me$_2$]C$_3$H$_4$}$_3$(thf)$_{1.5}$ provides enough access to *tert*-butylnitrile that it can insert four times into the metal-allyl bonds, yielding a *sec*-amido species (Figure 31).[78] The coordination geometry around yttrium includes an oxygen atom from coordinated thf, four nitrogen atoms from the amido ligands, and an N···H contact (2.49 Å) from an amido hydrogen.

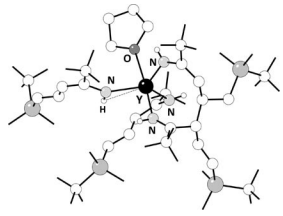

Figure 31. The structure of the nitrile insertion product from Y{1-[Si(*t*Bu)Me$_2$]C$_3$H$_4$}$_3$(thf)$_{1.5}$.

Multistep insertions are likely involved in the reaction between NiA′$_2$ and PMe$_3$, which yields tetramethyltetraphosphane, (MeP)$_4$. The product was identified with ^{1}H, ^{13}C, and ^{31}P NMR spectra and its formation studied with DFT methods.[17] Such studies suggest that the direct reaction NiA′$_2$ + PMe$_3$ → (η^3-A′)$_2$Ni(PMe$_3$) would not be favorable ($\Delta G°$ = +24.1 kcal mol^{-1}). For steric reasons, slippage of an allyl ligand from η^3 to η^1 would be required for phosphane binding. Subsequent additions of PMe$_3$ might then occur as the phosphane begins to demethylate, and P–P bond formation ensues.

A variety of f-element complexes with bulky allyl ligands function as polymerization catalysts; this may become a major area of application for these compounds. For example, La[A′]$_2$Cl(thf), Y[A′]$_2$Cl (which may actually be Y[A′]$_3$[73]) and Nd[A′]I$_2$(thf)$_{1.25}$ have been examined with several activators, including methylaluminoxane (MAO), as catalysts for the polymerization of 1,3-butadiene.[78] When activated with MAO, [1,3-(Si(*t*Bu)Me$_2$)$_2$C$_3$H$_3$]$_2$(Ti,Zr)(μ-Cl)$_2$Li(tmeda) and [1,3-(Si(*t*Bu)Me$_2$)$_2$C$_3$H$_3$]$_2$(Ti,Zr)Cl$_2$ are

polymerization catalysts for ethylene (forming high density polyethylene) and propylene (forming an elastomeric polypropylene with the Ti complexes and a stereoregular polymer with the Zr species).[13]

The cyclic $\{K(thf)_2Sm[A']_3\}_2$ is an effective single-component catalyst for the polymerization of methyl methacrylate (MMA) and ε-caprolactone; $Nd[A']_2I(thf)_2$ polymerizes ε-caprolactone with 85–95% conversion within a minute at 50 °C.[24] $[Ln\{(\eta^3\text{-}C_3H_3SiMe_3)_2SiMe_2\}_2\{\mu\text{-}K(thf)_x\}(thf)_y]_\infty$ (Ln = La, Y, Sc, Nd) and $[Li(OEt_2)_4][Sm\{(\eta^3\text{-}C_3H_3SiMe_3)_2SiMe_2\}_2]$ polymerize MMA without activation, and the yttrium compound displays turnover numbers at 0 °C of over 86,000 h^{-1}.[31]

Polymerization of MMA is also effected by the complexes $Eu[A']_2(thf)_2$, $Yb[A']_2(thf)_2$, $Ce[A']_3(thf)$, $Nd[A']_3(thf)$, $Sm[A']_2(thf)_2$ and $[Li(thf)_4][Ce\{A'\}_3I]$, all of which produce atactic polymethylmethacrylate (PMMA).[45] Among the neutral lanthanide allyl complexes, the polymerization activity appears to vary with the radius of the lanthanide metals and with the number of coordinated allyls; i.e., with the access of MMA to the metal centers. The divalent complexes $Sm[A']_2(thf)_2$ and $Eu[A']_2(thf)_2$, for example, which contain the larger metals samarium and europium ($Sm^{2+} \approx Eu^{2+}$ 1.17 Å for CN number 6),[85] have TOF values over ten times higher than $Yb[A']_2(thf)_2$ (Yb^{2+} = 1.02 Å for CN number 6). Conversely, the complexes containing trivalent cerium ($Ce[A']_3(thf)$) and neodymium ($Nd[A']_3(thf)$) have lower activity than any of the divalent species, probably reflecting the steric congestion around the smaller radii (Ce^{3+} 1.07 Å; Nd^{3+} 1.03 Å for CN 7).

An analysis of lanthanide allyl complexes that have been reported to polymerize MMA reveals that the potassium lanthanate complexes $K[Ln\{A'\}_4]$ are more efficient catalysts than the neutral complexes, and exhibit TOF values that are 10–100 times greater.[45] Interestingly, the potassium complex K[A′] displayed the highest TOF for MMA polymerization of all tested compounds (104,000 h^{-1}). Given its level of activity, it is possible that the increased effectiveness of the salt complexes stemmed from the presence of the alkali cations, a hypothesis supported by the higher TOF values that accompanied increased amounts of K[A′] in catalyst mixtures. Cation effects are recognized as important variables in anionic polymerization,[87] and the presence of alkali metal ions should be considered in studies of allyl lanthanide salt complexes in such polymerizations.

The homoleptic complexes MA'_2 (M = Cr, Fe, Co, Ni) have been tested as catalysts for the polymerization of norbornene.[88] Even when activated with methylaluminoxane (MAO), the Fe and Co compounds are only weakly active, but the Cr and Ni complexes are both active and generate high molecular weight poly(norbornene)s. This is rare behavior for any type of chromium catalyst. Ethylene was polymerized by CrA'_2 alone, and its activity was depressed by the presence of MAO. In contrast, a $CrA'_2/B(C_6F_5)_3$ mixture was active for ethylene polymerization but not for norbornene; NMR evidence suggests that the $B(C_6F_5)_3$ generates the $[CrA'_2]^+$ cation, which is presumably the active polymerization agent. Ethylene/norbornene copolymerization was possible in the $CrA'_2/B(C_6F_5)_3$ system, although the activity was low, and only limited norbornene insertion (11%) was observed.

Conclusions

It has been scarcely a decade since the chemistry of metal complexes containing sterically enhanced allyl ligands expanded beyond the organolithium compounds with which many of the ligands were originally associated. The increase in thermal and kinetic stability associated with the bulky ligands has allowed the synthesis of new types of compounds (e.g., CrA'_2), stabilized versions of known complexes (e. g, NiA'_2), the first structural authentication of mixed bonding modes in a single allyl complex (i.e., in $[MnA'_3]^-$) and has added cation-π bonding to the σ/π duality of allyl bonding (e.g., in $\{Mg[A']_2\}_2$).

There are certainly many challenges that lie ahead in the field of bulky allyl complexes. Synthetically, almost none of the second and third row transition metals are represented, even though in some cases the unsubstituted versions have been known for a long time [e.g., $Pd(C_3H_5)_2$, $Pt(C_3H_5)_2$]. A broader range of bulky substituents, including hydrocarbyl groups such as *i*Pr and *t*Bu, needs to be explored, as they will provide electronic features different from the trialkylsilyl groups that have served as the workhorses of the chemistry. Some of the polymerization reactions observed to date are promising, especially with the biologically compatible s-block metals, but considerable progress in improving stereocontrol will be needed to increase their attractiveness as practical initiators.

On the whole, however, the substituent chemistry already known demonstrates how much the chemistry of the "little" allyl ligand can "grow up" when augmented with bulky groups. Advancements in the coming years can be expected to be interesting indeed.

Acknowledgments

The US National Science Foundation (CHE-0616880) and the American Chemical Society – Petroleum Research Fund are thanked for support of the research from my laboratory. I am also grateful to the students who have contributed to allyl research, and whose names are listed as co-authors in papers cited throughout this review. The reviewers are thanked for helpful comments.

[1] C. Elschenbroich, *Organometallics*, 3rd ed., Wiley-VCH, Weinheim, **2006**.
[2] L. S. Hegedus, *Transition Metals in the Synthesis of Complex Organic Molecules*, 2nd ed., University Science Books, Sausalito, California, **1999**.
[3] G. Wilke, B. Bogdanovic, P. Hardt, P. Heimbach, W. Keim, M. Kroner, W. Oberkirch, K. Tanaka, D. Walter, *Angew. Chem. Int. Ed. Engl.* **1966**, *5*, 151–164.
[4] M. L. Hays, T. P. Hanusa, *Adv. Organomet. Chem.* **1996**, *40*, 117–170.
[5] T. P. Hanusa, *Organometallics* **2002**, *21*, 2559–2571.
[6] P. Jutzi, N. Burford, *Chem. Rev.* **1999**, *99*, 969–990.
[7] J. M. Grosselin, P. H. Dixneuf, *J. Organomet. Chem.* **1986**, *314*, C76–C80.

[8] A. Schott, H. Schott, G. Wilke, J. Brandt, H. Hoberg, E. G. Hoffmann, *Justus Liebigs Ann. Chem.* **1973**, 508–530.
[9] G. Fraenkel, A. Chow, W. R. Winchester, *J. Am. Chem. Soc.* **1990**, *112*, 1382–1386.
[10] G. Fraenkel, A. Chow, W. R. Winchester, *J. Am. Chem. Soc.* **1990**, *112*, 2582–2585.
[11] G. Boche, G. Fraenkel, J. Cabral, K. Harms, N. J. R. van Eikema Hommes, J. Lohrenz, M. Marsch, P. v. R. Schleyer, *J. Am. Chem. Soc.* **1992**, *114*, 1562–1565.
[12] G. Fraenkel, W. R. Winchester, *Organometallics* **1990**, *9*, 1314–1316.
[13] B. Ray, T. G. Neyroud, M. Kapon, Y. Eichen, M. S. Eisen, *Organometallics* **2001**, *20*, 3044–3055.
[14] These volumes were calculated at the B3LYP/6-31+G(d) level, using the MacSpartan program (T. Hanusa, unpublished results).
[15] S. Harder, M. Lutz, A. W. G. Straub, *Organometallics* **1997**, *16*, 107–113.
[16] C. N. Carlson, J. D. Smith, T. P. Hanusa, W. W. Brennessel, V. G. Young Jr., *J. Organomet. Chem.* **2003**, *683*, 191–199.
[17] K. T. Quisenberry, J. D. Smith, M. Voehler, D. F. Stec, T. P. Hanusa, W. W. Brennessel, *J. Am. Chem. Soc.* **2005**, *127*, 4376–4387.
[18] C. N. Carlson, T. P. Hanusa, W. W. Brennessel, *J. Am. Chem. Soc.* **2004**, *126*, 10550–10551.
[19] C. K. Gren, T. P. Hanusa, A. L. Rheingold, *Main Group Chem.* **2009**, *8*, 225–235.
[20] J. D. Smith, T. P. Hanusa, V. G. Young Jr., *J. Am. Chem. Soc.* **2001**, *123*, 6455–6456.
[21] J. D. Smith, K. T. Quisenberry, T. P. Hanusa, W. W. Brennessel, *Acta Crystallogr., Sect. C* **2004**, *60*, m507–m508.
[22] M. Schormann, S. Garratt, M. Bochmann, *Organometallics* **2005**, *24*, 1718–1724.
[23] C. J. Kuehl, C. K. Simpson, K. D. John, A. P. Sattelberger, C. N. Carlson, T. P. Hanusa, *J. Organomet. Chem.* **2003**, *683*, 149–154.
[24] T. J. Woodman, M. Schormann, D. L. Hughes, M. Bochmann, *Organometallics* **2003**, *22*, 3028–3030.
[25] T. P. Hanusa, C. N. Carlson, in *Encyclopedia of, Inorg. Chem. II, Vol. 9* (Ed.: R. B. King), Wiley, **2005**, pp. 5690–5695.
[26] C. F. Caro, M. F. Lappert, P. G. Merle, *Coord. Chem. Rev.* **2001**, *219–221*, 605–663.
[27] M. Sudupe, J. s. Cano, P. Royo, E. Herdtweck, *Eur. J. Inorg. Chem.* **2004**, *2004*, 3074–3083.
[28] C. Strohmann, K. Lehmen, S. Dilsky, *J. Am. Chem. Soc.* **2006**, *128*, 8102–8103.
[29] K. T. Quisenberry, C. K. Gren, R. E. White, T. P. Hanusa, W. W. Brennessel, *Organometallics* **2007**, *26*, 4354–4356. The rubidium chemistry is described in footnote 10.
[30] R. Fernandez-Galan, P. B. Hitchcock, M. F. Lappert, A. Antinolo, A. M. Rodriguez, *J. Chem. Soc., Dalton Trans.* **2000**, 1743–1749.
[31] T. J. Woodman, M. Schormann, M. Bochmann, *Organometallics* **2003**, *22*, 2938–2943.
[32] P. B. Hitchcock, M. F. Lappert, W.-P. Leung, D.-S. Liu, T. C. W. Mak, Z.-X. Wang, *J. Chem. Soc., Dalton Trans.* **1999**, 1257–1262.
[33] S. A. Solomon, C. A. Muryn, R. A. Layfield, *Chem. Commun.* **2008**, 3142–3144.
[34] G. Fraenkel, J. Cabral, X. Chen, A. Chow, *J. Org. Chem.* **2009**, *74*, 2311–2320.
[35] G. Fraenkel, J. A. Cabral, *J. Am. Chem. Soc.* **1993**, *115*, 1551–1557.
[36] G. Fraenkel, F. Qiu, *J. Am. Chem. Soc.* **1996**, *118*, 5828–5829.
[37] G. Fraenkel, F. Qiu, *J. Am. Chem. Soc.* **1997**, *119*, 3571–3579.
[38] G. Fraenkel, J. H. Duncan, J. Wang, *J. Am. Chem. Soc.* **1998**, *121*, 432–443.
[39] G. Fraenkel, A. Chow, R. Fleischer, H. Liu, *J. Am. Chem. Soc.* **2004**, *126*, 3983–3995.
[40] R. E. White, T. P. Hanusa, B. E. Kucera, *J. Am. Chem. Soc.* **2006**, *128*, 9622–9623.
[41] W. R. Winchester, W. Bauer, P. v. R. Schleyer, *J. Chem. Soc., Chem. Commun.* **1987**, 177–179.
[42] C. Praesang, Y. Sahin, M. Hofmann, G. Geiseler, W. Massa, A. Berndt, *Eur. J. Inorg. Chem.* **2004**, 3063–3073.
[43] G. Boche, H. Etzrodt, M. Marsch, W. Massa, G. Baum, H. Dietrich, W. Mahdi, *Angew. Chem. Int. Ed. Engl.* **1986**, *25*, 104–105.
[44] R. A. Layfield, F. Garcia, J. Hannauer, S. M. Humphrey, *Chem. Commun.* **2007**, 5081–5083.
[45] C. K. Simpson, R. E. White, C. N. Carlson, D. A. Wrobleski, C. J. Kuehl, T. A. Croce, I. M. Steele, B. L. Scott, T. P. Hanusa, A. P. Sattelberger, K. D. John, *Organometallics* **2005**, *24*, 3685–3691.
[46] M. J. Harvey, T. P. Hanusa, M. Pink, *J. Chem. Soc., Dalton Trans.* **2001**, 1128–1130.
[47] E. A. Hill, W. A. Boyd, H. Desai, A. Darki, L. Bivens, *J. Organomet. Chem.* **1996**, *514*, 1–11.
[48] S. C. Chmely, C. N. Carlson, T. P. Hanusa, A. L. Rheingold, *J. Am. Chem. Soc.* **2009**, *131*, 6344–6345.
[49] C. K. Gren, T. P. Hanusa, W. W. Brennessel, *Polyhedron* **2006**, *25*, 286–292.
[50] D. Vijay, G. N. Sastry, *Phys. Chem. Chem. Phys.* **2008**, *10*, 582–590.
[51] A. S. Reddy, G. N. Sastry, *J. Phys. Chem. A* **2005**, *109*, 8893–8903.
[52] J. Cheng, W. Zhu, Y. Tang, Y. Xu, Z. Li, K. Chen, H. Jiang, *Chem. Phys. Lett.* **2006**, *422*, 455–460.
[53] A. S. Reddy, H. Zipse, G. N. Sastry, *J. Phys. Chem. B* **2007**, *111*, 11546–11553.
[54] M. J. Harvey, T. P. Hanusa, V. G. Young Jr., *Angew. Chem. Int. Ed.* **1999**, *38*, 217–219.
[55] R. A. Williams, T. P. Hanusa, J. C. Huffman, *Organometallics* **1990**, *9*, 1128–1134.
[56] A. E. Smith, *Inorg. Chem.* **1972**, *11*, 165–170.
[57] N. W. Murrall, A. J. Welch, *J. Organomet. Chem.* **1986**, *301*, 109–130.
[58] C. K. Gren, T. P. Hanusa, A. L. Rheingold, *Organometallics* **2007**, *26*, 1643–1649.
[59] J. Cheon, L. H. Dubois, G. S. Girolami, *Chem. Mater.* **1994**, *6*, 2279–2287.
[60] I. Fernández, E. Martinez-Viviente, F. Breher, P. S. Pregosin, *Chem. Eur. J.* **2005**, *11*, 1495–1506.
[61] G. C. Forbes, A. R. Kennedy, R. E. Mulvey, B. A. Roberts, R. B. Rowlings, *Organometallics* **2002**, *21*, 5115–5121.
[62] M. S. Kralik, L. Stahl, A. M. Arif, C. E. Strouse, R. D. Ernst, *Organometallics* **1992**, *11*, 3617–3621.
[63] T. Aoki, A. Furusaki, Y. Tomie, K. Ono, K. Tanaka, *Bull. Chem. Soc. Jpn.* **1969**, *42*, 545–547.
[64] R. A. Layfield, S. M. Humphrey, *Angew. Chem. Int. Ed.* **2004**, *43*, 3067–3069.
[65] M. E. Switzer, R. Wang, M. F. Rettig, A. H. Maki, *J. Am. Chem. Soc.* **1974**, *96*, 7669–7674.
[66] R. A. Layfield, M. Buehl, J. M. Rawson, *Organometallics* **2006**, *25*, 3570–3575.
[67] A. Fürstner, R. Martin, H. Krause, G. Seidel, R. Goddard, C. W. Lehmann, *J. Am. Chem. Soc.* **2008**, *130*, 8773–8787.
[68] H. Bönnemann, B. Bogdanovic, G. Wilke, *Angew. Chem. Int. Ed. Engl.* **1967**, *6*, 804.
[69] L. S. Hegedus, D. H. P. Thompson, *J. Am. Chem. Soc.* **1985**, *107*, 5663–5669.
[70] R. Taube, H. Windisch, S. Maiwald, H. Hemling, H. Schumann, *J. Organomet. Chem.* **1996**, *513*, 49–61.
[71] R. E. White, T. P. Hanusa, B. E. Kucera, *J. Organomet. Chem.* **2007**, *692*, 3479–3485.
[72] T. J. Woodman, M. Schormann, D. L. Hughes, M. Bochmann, *Organometallics* **2004**, *23*, 2972–2979.
[73] R. E. White, T. P. Hanusa, *Organometallics* **2006**, *25*, 5621–5630.

[74] M. Horácek, J. Hiller, U. Thewalt, M. Polášek, K. Mach, *Organometallics* **1997**, *16*, 4185–4191.
[75] J. A. Pool, E. Lobkovsky, P. J. Chirik, *J. Am. Chem. Soc.* **2003**, *125*, 2241–2251.
[76] A. Eisenstadt, A. Efraty, *Organometallics* **1982**, *1*, 1100–1101.
[77] E. Ihara, K. Koyama, H. Yasuda, N. Kanehisa, Y. Kai, *J. Organomet. Chem.* **1999**, *574*, 40–49.
[78] T. J. Woodman, M. Schormann, M. Bochmann, *Isr. J. Chem.* **2002**, *42*, 283–293.
[79] J. M. Veauthier, E. J. Schelter, C. J. Kuehl, A. E. Clark, B. L. Scott, D. E. Morris, R. L. Martin, J. D. Thompson, J. L. Kiplinger, K. D. John, *Inorg. Chem.* **2005**, *44*, 5911–5920.
[80] C. J. Kuehl, R. E. Da Re, B. L. Scott, D. E. Morris, K. D. John, *Chem. Commun.* **2003**, 2336–2337.
[81] R. E. Da Re, C. J. Kuehl, M. G. Brown, R. C. Rocha, E. D. Bauer, K. D. John, D. E. Morris, A. P. Shreve, J. L. Sarrao, *Inorg. Chem.* **2003**, *42*, 5551–5559.
[82] S. C. Sockwell, T. P. Hanusa, *Inorg. Chem.* **1990**, *29*, 76–80.
[83] K. N. Raymond, C. W. Eigenbrot, *Acc. Chem. Res.* **1980**, *13*, 276–283.
[84] J. L. Atwood, W. E. Hunter, A. L. Wayda, W. J. Evans, *Inorg. Chem.* **1981**, *20*, 4115–4119.
[85] R. D. Shannon, *Acta Crystallogr., Sect. A* **1976**, *32*, 751–767.
[86] S. Harder, *Angew. Chem. Int. Ed.* **2004**, *43*, 2714–2718.
[87] M. Kawalec, M. Smiga-Matuszowicz, P. Kurcok, *Eur. Polym. J.* **2008**, *44*, 3556–3563.
[88] T. J. Woodman, Y. Sarazin, S. Garratt, G. Fink, M. Bochmann, *J. Mol. Catal. A* **2005**, *235*, 88–97.

Received: August 19, 2009
Published Online: February 23, 2010

